

Adaptive Normal-Boundary Intersection Directions for Evolutionary Many-objective Optimization with Complex Pareto Fronts

Maha Elarbi¹, Slim Bechikh¹, and Carlos A. Coello Coello²

¹ SMART Lab, ISG, University of Tunis, Tunisia

`arbi.maha@yahoo.com`, `slim.bechikh@fsegn.rnu.tn`

² Departamento de Computacion, CINVESTAV-IPN, Mexico City, Mexico

`ccoello@cs.cinvestav.mx`

Abstract. Decomposition-based Many-Objective Evolutionary Algorithms (MaOEAs) usually adopt a set of pre-defined distributed weight vectors to guide the solutions towards the Pareto optimal Front (PF). However, when solving Many-objective Optimization Problems (MaOPs) with complex PFs, the effectiveness of MaOEAs with a fixed set of weight vectors may deteriorate which will lead to an imbalance between convergence and diversity of the solution set. To address this issue, we propose here an Adaptive Normal-Boundary Intersection Directions Decomposition-based Evolutionary Algorithm (ANBID-DEA), which adaptively updates the Normal-Boundary Intersection (NBI) directions used in MP-DEA. In our work, we assist the selection mechanism by progressively adjusting the NBI directions according to the distribution of the population to uniformly cover all the parts of the complex PFs (i.e., those that are disconnected, strongly convex, degenerate, etc.). Our proposed ANBID-DEA is compared with respect to five state-of-the-art MaOEAs on a variety of unconstrained benchmark problems with up to 15 objectives. Our results indicate that ANBID-DEA has a competitive performance on most of the considered MaOPs.

Keywords: Many-objective optimization · Decomposition-based algorithms · Adaptive normal-boundary intersection directions

1 Introduction

Many real-world optimization problems normally have more than three (often conflicting) objectives. For example: Cloud task scheduling [31] and protein structure prediction [30], to mention just a few. These are the so-called Many-objective Optimization Problems (MaOPs). Researchers have shown that the conventional Multi-objective Evolutionary Algorithms (MOEAs) face some difficulties when the number of objectives increases mainly because the Pareto dominance relationship is not able to properly differentiate solutions [5]. Solutions quickly become non-dominated as we add more objectives and, consequently, the selection pressure dilutes, which prevents the algorithm from properly converging to the true Pareto optimal Front (PF). Several Many-Objective Evolutionary

Algorithms (MaOEAs) have been proposed over the years. They can be roughly classified into the following four categories [9]: (1) Dominance relation-based MaOEAs, (2) indicator-based MaOEAs, (3) objective reduction-based MaOEAs, and (4) decomposition-based MaOEAs. The latter decompose the problem into a number of sub-problems that are then simultaneously optimized with the help of weight vectors (i.e., reference points). The work reported here will focus on this last category.

Decomposition-based algorithms have attracted a lot of interest and they are considered as one of the most promising options for handling MaOPs. MOEA/D [29] and NSGA-III [4] are the most representative decomposition-based algorithms and they are designed to perform well on high dimensional objective problems. However, they face several challenges in providing well-diversified solutions particularly when the problem complexity increases (i.e., in the presence of a large number of objectives and/or complicated PF shapes).

One interesting choice is to explore the merits of combining Pareto dominance and decomposition. A representative approach of such type is the Multi-objective Evolutionary Algorithm Based on Dominance and Decomposition (MOEA/DD) [13]. MOEA/DD favors the selection of non-dominated solutions over dominated ones and emphasizes the selection of solutions in isolated regions since these solutions are beneficial to maintain the population's diversity. The updating mechanism of MOEA/DD has shown its effectiveness in solving problems having regular PFs. Nevertheless, MOEA/DD does not provide a well-diversified set of solutions on some problems with irregular PF shapes (i.e., problems with degenerate, discontinuous, inverted, strongly convex, and/or strongly concave fronts). In fact, when we use pre-defined weight vectors, several weight search directions may miss several regions of the irregular PF. Since the performance of the decomposition-based algorithms that were originally proposed depends on the pre-defined set of reference points, they achieve promising performance on MaOPs with regular PFs, but the uniformity of the distribution of the solutions cannot be guaranteed with irregular PFs. To overcome this shortcoming, some authors have proposed to adapt the weight vectors during the evolutionary search process. Many adaptive weight vector-based algorithms have been proposed, such as MOEA/D-LTD [25] and ADEA [1]. VaEA eliminates the use of weight vectors and uses the solutions themselves as reference directions [26]. This approach uses a modified niche preservation operator that incorporates the worse-elimination and the maximum-vector-angle-first principles to balance between convergence and diversity. Nevertheless, VaEA emphasizes diversity and it is difficult for this algorithm to achieve good convergence in some MaOPs with regular PFs.

Motivated by the previously discussed issues of MOEA/DD and VaEA, we propose here a new Adaptive Normal Boundary Intersection Directions Decomposition-based Evolutionary Algorithm (ANBID-DEA) for MaOPs. ANBID-DEA adaptively updates the set of pre-defined Normal Boundary Intersection (NBI) directions employed in MP-DEA during the evolutionary process [6], favors the selection of isolated solutions as done in the update procedure of MOEA/DD, and integrates the mechanisms used in the worse-elimination

principle of VaEA. The main contributions of this paper can be summarized as follows:

1. We propose ANBID-DEA that aims to enhance the update procedure of MOEA/DD and the worse-elimination mechanism of VaEA by ensuring the balance between the uniformity of the distribution of the solutions and the convergence when dealing with irregular PFs.
2. We investigate the importance of adaptively adjusting the NBI directions used in MP-DEA according to the distribution of the population to discover the missing parts of the PF and to detect misleading directions.
3. We show that ANBID-DEA is able to outperform several state-of-the-art approaches in terms of IGD and HV when applied to a variety of unconstrained benchmark problems.

The remainder of this paper is organized as follows. Section 2 introduces the previous related work and the main motivation for this research. In Section 3, we describe our proposed ANBID-DEA. Section 4 presents our experimental setup. In Section 5, we present the performance assessment of our proposed ANBID-DEA by comparing it to five MaOEAs. Section 6 provides our conclusions and some possible paths for future research.

2 Previous Related Work and Motivation

Most of the MaOEAs which belong to the first generation of decomposition-based algorithms follow the general assumption which states that evenly distributed weights result in an evenly distributed solution set [12]. Nevertheless, when facing problems with irregular PFs (i.e., disconnected, degenerated, strongly convex, etc.) it is hard to estimate the shape of the PF using a set of static distributed weights, since several weights may not intersect the PF. Therefore, researchers have proposed to dynamically adjust the weight directions during the search process to adapt the shape of the target PF according to the current population. In the literature, several attempts have been made in this direction. Recently, several works tended to consider the distribution of the current population during the evolutionary process when adjusting weights [18]. Some weight adaptation methods use the distribution of the solutions to guide the adaptation of weights, while other methods employ some solutions in the population to generate weights. Representative algorithms include A-NSGA-III [11], VaEA [26], MOEA/D-AM2M [15], and MaOEA-PDE [27]. Other existing approaches use an external solution set (i.e., an external archive) to preserve the best solutions from the population. These approaches utilize the preserved solutions in two manners: (1) using the archive to generate weights (such as in iRVEA [16], MOEA/D-AWA [19], and AdaW [14]) or (2) leveraging the solutions from the archive to estimate the shape of the PF and to guide the weight adaptation process (such as in RVEA-iGNG [17] and MOEA/D-SOM [8]). The main advantage of using an archive is that it is able to provide a robust representation of

the PF shape by guiding the weight adaptation process. For more details on the proposed weight vector adaptation methods, refer to [18].

Although the aforementioned weight vector adaptation methods have shown good performance, three main issues remain. First, some of the previously mentioned methods adapt multiple weights at a single generation and at any time in the evolutionary process. However, as shown in [7], the frequent change of the weights may deteriorate the convergence of the solutions. Second, an unstable archive in which we perform changes on its solutions may harm the convergence of the weight adaptation algorithms [18]. Third, to the best of our knowledge all the existing adaptation methods adjust PBI directions (i.e., a line connecting the origin and a weight vector). Such directions are well-suited to solve MaOPs with regular PFs. However, when the shape of the PF is irregular, PBI-based adaptation methods struggle to provide a set of well-distributed solutions due to the inconsistencies between the shape of the PF and the distribution of the PBI directions [6,21].

The limitation of the existing weight adaptation methods motivated us to propose ANBID-DEA which replaces only one weight at a time. Moreover, we also propose an enhanced worse-elimination strategy that: (1) eliminates the worst solutions in terms of convergence and diversity and replaces them by better ones and (2) updates the NBI directions during the search process so that they uniformly intersect with the PF regardless of the complexity of its geometrical shape.

3 Our Proposed Approach: ANBID-DEA

3.1 General Framework

ANBID-DEA follows the same framework of MOEA/DD but it modifies its update mechanism. First, a population P of size N and a set of W well-spread reference points RP are generated. Then, a set of mirror points MP is generated so that each reference point in RP has its mirror point in MP . The RP and MP sets are used to create the NBI directions. After that, the loop iteration is executed until the termination criterion is met. A reproduction procedure is applied to generate offspring solutions by performing the mating selection and the variation operation. The mating selection is applied to choose the mating parents, while the variation operation generates new candidate solutions. The created offspring solutions are used to update the population P by considering an offspring solution x_c each time. Once the offspring solution x_c is added to P , we obtain a new population P' with size $N + 1$. Thereafter, we normalize the members of the P' population and we associate the solutions to their closest reference points by computing the acute angle between each solution and the reference points. After this, we apply non-dominated sorting to divide the population into different layers using Pareto dominance. Finally, we apply our enhanced worse-elimination mechanism to delete an inferior solution.

3.2 Construction of the NBI Directions

The generation of the reference points set RP is done using the two-layer generation method suggested in [13]. Using this method, an RP set with W well-distributed reference points is obtained and intermediate reference points within the simplex are guaranteed. Thereafter, the set of W mirror points MP is created using the same mirror points generation procedure employed in [6]. The latter constructs a set of mirror points by decreasing the coordinates of the reference points by 1. The obtained reference and mirror points are then used to create the NBI directions that connect each reference point with its corresponding mirror version.

3.3 Generation of the Offspring Solutions

The generation of offspring solutions takes place in two steps. First, mating selection is performed in which parents are chosen at random from the population. The second step is the variation operation. In this operation, genetic operators are applied on the mating parents. The operators used in our approach are the well-known Simulated Binary Crossover (SBX) and polynomial-based mutation. The SBX operator uses two parents to create two offspring solutions. This operator uses the distribution index parameter that is responsible for creating an offspring close or away from its parents.

3.4 Normalization and Association of the Solutions

After the creation of the P' population, we then normalize its members. This step is important specially when we deal with MaOPs having disparately scaled PFs. Thus, the objective value (i.e., $f_i, i = 1, \dots, M$) of each solution x is normalized through the following equation:

$$f'_i(x) = \frac{f_i(x) - z_i^*}{z_i^{nad} - z_i^*} \quad (1)$$

where z_i^* and z_i^{nad} are the ideal and the nadir points of the population P' , respectively. z_i^* corresponds to the minimum value of f_i , while z_i^{nad} is the i^{th} objective value of the nadir point z^{nad} . For the estimation of z^{nad} , we use the same method employed in [28]. We first determine the extreme solution corresponding to each coordinate axis (i.e., f_j) by minimizing an Achievement Scalarizing Function (ASF). Then, we construct an M -dimensional hyperplane by connecting the extreme solutions. Next, the interception $a_i, i = 1, \dots, M$ of the hyperplane with each objective axis is determined. Finally, the objective values of each solution are normalized using equation (1), where $z_i^{nad} - z_i^* = a_i$ is used and the value of z_i^{nad} is updated. For a degenerate PF, we may not be able to determine the extreme solutions that will serve to construct the hyperplane. In such a case, z_i^{nad} is assigned as the maximum value of each objective f_i for all solutions, where $i = 1, \dots, M$.

After normalizing the solutions, each solution x is associated with a unique sub-region (i.e., reference direction) according to its acute angle value that is computed as follows:

$$\text{angle}(x, RP_j) \triangleq \arccos \left| \frac{F'(x) \bullet RP_j}{\text{norm}(x) \cdot \text{norm}(RP_j)} \right| \quad (2)$$

where $F'(x) = (f'_1(x), f'_2(x), \dots, f'_M(x))^T$, $RP_j = (rp_{j,1}, rp_{j,2}, \dots, rp_{j,M})^T$, $\text{norm}(x) \triangleq \sqrt{\sum_{i=1}^M f'_i(x)^2}$, $F'(x) \bullet RP_j$ returns the inner product between $F'(x)$ and RP_j , and it is defined as follows:

$$F'(x) \bullet RP_j = \sum_{i=1}^M f'_i(x) \cdot rp_{j,i} \quad (3)$$

A solution is associated to the reference point that has the smallest angle with it. In this manner, we can identify three types of reference directions: (1) reference directions that are not associated by any solution, (2) isolated reference directions with a single solution associated to them, and (3) crowded reference directions that are associated with more than one solution.

3.5 Enhanced Worse-Elimination Selection

Once the population members are associated to the reference directions, we apply non-dominated sorting to divide the population members into different levels using Pareto dominance. Next, we eliminate an inferior solution x from P' by following one of these two scenarios:

1. *Case 1: There is a single non-domination level (i.e., $l = 1$):* We start by identifying the non-isolated solution x having the minimum angle with its reference point:
 - (a) If this angle is non-zero and less than σ , then the following steps are executed: (1) the solution x is eliminated, (2) the reference vector takes the direction of the solution y that has the maximum angle with it, (3) a new NBI direction is generated by creating the mirror point y' of the solution y , (4) and the solutions are re-associated using the new set of reference points. Fig. 1 illustrates this case where the non-dominated solution x is deleted and the NBI direction of x is replaced by generating a new NBI direction (i.e., the line connecting the solution y and its new generated mirror point y').
 - (b) Otherwise, if the angle is greater than σ , we identify the most crowded sub-region and we delete the solution x having the highest Euclidean distance to its corresponding mirror point.
2. *Case 2: There are multiple non-domination levels (i.e., $l > 1$):* We identify the last layer F_l :

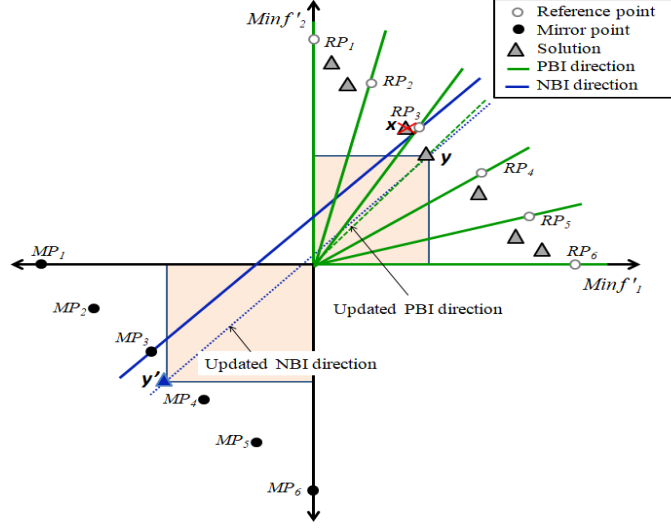


Fig. 1: Illustration of case 1(a) of the enhanced worse-elimination selection.

- (a) If it contains only isolated solutions, we delete the solution x having the highest Euclidean distance to its corresponding mirror point in the most crowded sub-region.
- (b) Otherwise, we look for the non-isolated solution x in F_l that has the minimum angle with its reference point and we perform the same steps of case 1.

In this work, $\sigma = \frac{\pi \div 2}{N+1}$ as set in [26]. It is important to note that the angle represents a metric of diversity and, in some cases, also of convergence, while the Euclidean distance measures uniformity and convergence. Moreover, our enhanced worse-elimination selection mechanism adaptively updates the NBI directions during the evolutionary process to uniformly cover the irregular PFs and eliminates the worst solutions in terms of convergence and diversity through the use of the PBI (acute angle) and NBI (Euclidean distance) metrics (cf. Fig. 2).

4 Experimental Study

4.1 Benchmark Problems

In order to assess the performance of our proposed ANBID-DEA, we adopted the benchmarks used in the original papers of the algorithms from our comparative study: The three well-known test suites DTLZ, WFG, and MaF [13,6]. These test problems have several challenging features. In this paper, we have selected only the test problems DTLZ1-4, WFG2-3, WFG5, WFG9, MaF1, MaF3, and MaF6-7. The considered instances cover the following properties: linear, multi-modal, concave, convex, scaled, degenerate, deceptive, inverted, disconnected,

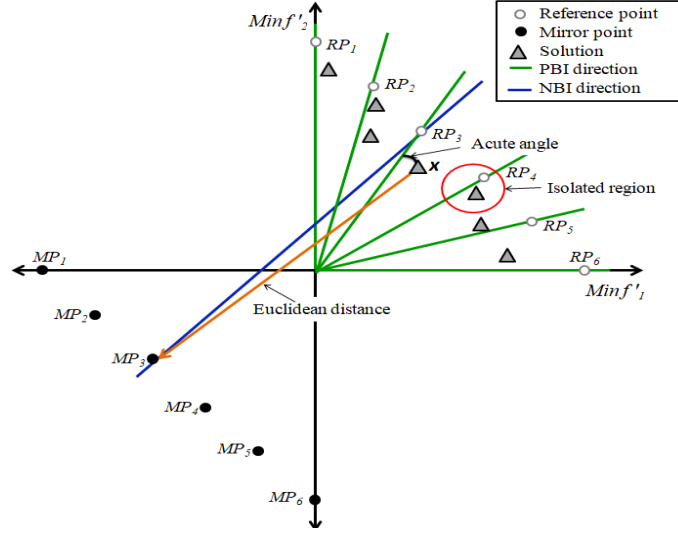


Fig. 2: Illustration of the acute angle and Euclidean distance metrics.

mixed, and biased. In this paper, the number of objectives varies from 5 to 15, $M \in \{5, 10, 15\}$. The number of decision variables was set to $D = M + k - 1$, where k is set as 5 for DTLZ1 and 10 for DTLZ2-4. For the considered WFG test problems, the number of decision variables was set as $D = 2 \times (M - 1) + 20$. The MaF problems have the same number of decision variables as in DTLZ. For MaF1, MaF3, and MaF6, $k = 10$, while for MaF7, $k = 20$.

4.2 Baseline Approaches

We have compared the performance of our proposed ANBID-DEA with respect to that of two non-adaptive weight vector-based algorithms: MP-DEA (i.e., the fixed NBI direction-based algorithm version of ANBID-DEA) [6], and MOEA/DD [13]. Moreover, we have also conducted comparative experiments against three adaptive-based algorithms: VaEA [26] which uses the maximum-vector-angle-first rule to select individuals one by one as a reference direction, RVEA [3] that uses an adaptive strategy for reference vectors and an angle penalized distance to balance the convergence and diversity of the solutions in a high-dimensional objective space, and MOEA/D-AWA [19] that adds and deletes weights according to the sparsity degree of the solutions stored in the archive.

4.3 Performance Measures

To assess the performance of the six approaches adopted in our comparative study, we used the Inverted Generational Distance (IGD) [2] and the HyperVolume (HV) [32] performance measures since they are both commonly used in the specialized literature.

Table 1: Specific experimental parameters settings.

Algorithm	Parameter	Value
RVEA	Changing rate α of the penalty function	2
	Adaptive reference vector update frequency f_r	0.1
MOEA/D-AWA	Maximum capacity of the archive	$1.5N$
	Maximum number of adjusted sub-problems nus	$rate_update_weight \times N$
	$rate_update_weight$	0.05
MOEA/DD	$rate_evol$	0.8
	Penalty parameter θ of PBI	5.0
	Number T of neighbors	20
	probability δ of selecting a neighbor	0.9

- IGD calculates the distance between the set of non-dominated solutions obtained on the final population (S) and a reference set (normally, the true Pareto front of the problem). The lower the IGD value is, the better the quality of S . The reference set is generated using the open-source platform PlatEMO [24].
- HV computes the volume covered by the set of non-dominated solutions obtained on the final population with respect to a specified reference point. It measures both convergence and maximum spread. As recommended in [26] the reference point was set to 1.1 times of the upper bounds of the true PFs. The larger the HV value is, the better the quality of S .

4.4 Parameters Settings and Statistical Testing

A parameter tuning process was conducted to find the best parameter values for each algorithm. In all the experiments, each algorithm was run 31 times on each test instance. The population sizes of MP-DEA, VaEA, and RVEA were set as 212, 276, and 136 for $M = 5$, $M = 10$, and $M = 15$, respectively. For ANBID-DEA, MOEA/DD, and MOEA/D-AWA the population size was set to 210 for $M = 5$, 275 for $M = 10$, and 135 for $M = 15$. The number of weight vectors was set the same as the population size of MOEA/DD. SBX and polynomial-based mutation were used to produce new offspring solutions. The crossover probability and the mutation probability were set to 1.0 and $1/D$, respectively. The distribution index of SBX was set to 30, while the distribution index of the polynomial-based mutation operator was set to 20. In this paper, we used as a termination criterion a Maximum number of Function Evaluations (MFEs) for each algorithm. The MFEs were set as $MFEs = MaxGen \times N$, where MFE is equal 100.000 for $M = \{5, 10, 15\}$. Table 1 shows the settings of some specific parameters. In order to statistically compare the performance of the peer algorithms and to see whether there are statistical differences in their obtained results, we used the Friedman and Iman-Davenport statistical tests [23]. We have also applied the Wilcoxon test in a pairwise manner with a significance level of 0.05 [23]. The “+”, “-”, and “=” mean that the IGD or HV values of the considered algorithms are significantly better, significantly worse than, or without a significant difference to those of our proposed ANBID-DEA, respectively.

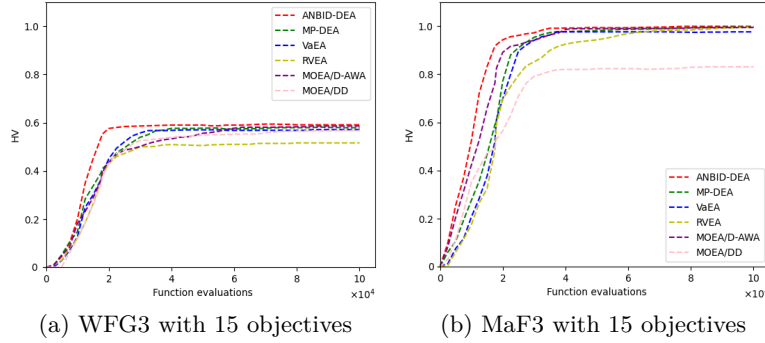


Fig. 3: Median HV variation curves of 31 independent runs performed by each algorithm on WFG3 and MaF3.

5 Results and Discussion

Table 2 shows the median IGD and HV results obtained on DTLZ1-4, WFG2-3, WFG5, WFG9, MaF1, MaF3, and MaF6-7. The statistical significance of the difference in results between our proposed ANBID-DEA and the peer algorithms is also shown by using the Wilcoxon test. We can see that ANBID-DEA had the best overall performance in almost all the considered test problems in terms of IGD and HV. MP-DEA had the second best performance and was very competitive with respect to ANBID-DEA, while VaEA ranked third and was able to obtain the second best performance on: (1) DTLZ2, MaF3, and MaF7 with 10, 5, and 10 objectives in terms of IGD, respectively and (2) the 5-objective version of MaF3 and the 10-objective version of MaF6 in terms of HV. MOEA/D-AWA, RVEA, and MOEA/DD had the worst position in the ranking. The performance of MOEA/D-AWA was promising on WFG3, MaF6, and MaF7 which have complex PF shapes (degenerate, disconnected, multi-modal, etc.). RVEA managed to obtain the best performance in the 5-objective version of MaF3 with respect to the IGD and HV indicators. Regarding MOEA/DD, it had a poor performance in almost all the considered test instances except for the 5- and 15-objective instances of DTLZ1 and MaF1, respectively. Fig. 3 shows the median HV values of each algorithm over the total number of function evaluations on WFG3 and MaF3 with 15 objectives. It can be seen from these figures that the median of ANBID-DEA converges faster than the other algorithms and remains stable at the maximum value. This can be explained by the fact that our approach is able to cover the different parts of the PF since the early stages of the search due to the application of its enhanced worse-elimination selection mechanism.

As can be seen from Table 2, our proposed ANBID-DEA shows a superior performance. ANBID-DEA significantly outperforms MP-DEA, VaEA, RVEA, MOEA/D-AWA, and MOEA/DD on 33, 36, 34, 34, and 36 problems from a total of 36 test instances in terms of IGD. Similar to the previous observation, ANBID-DEA significantly outperforms the other baseline approaches on 33, 35,

Table 2: Median values of IGD and HV on DTLZ1-4, WFG2-3, WFG5, WFG9, MaF1, MaF3, and MaF6-7. The first line shows the IGD value, while the second line indicates the HV value. The best and the second best results for each test instance are shown in boldface and underlined, respectively.

Problem	M	ANBID-DEA	MP-DEA	VaEA	RVEA	MOEA/D-AWA	MOEA/DD
DTLZ1	5	2.002E-1	2.430E-1 (-)	2.089E-1 (-)	2.336E-1 (-)	3.382E-1 (-)	2.005E-1 (-)
		1.00E+0	9.98E-1 (-)	9.88E-1 (-)	9.95E-1 (-)	9.83E-1 (-)	9.99E-1 (-)
	10	1.887E-1	1.893E-1 (-)	2.046E-1 (-)	1.915E-1 (-)	1.895E-1 (-)	2.864E-1 (-)
		1.09E+0	1.07E+0 (-)	9.94E-1 (-)	1.00E+0 (-)	1.06E+0 (-)	9.23E-1 (-)
	15	1.723E-1	<u>1.752E-1 (-)</u>	2.185E-1 (-)	2.085E-1 (-)	1.761E-1 (-)	1.832E-1 (-)
		1.08E+0	1.06E+0 (-)	9.97E-1 (-)	9.98E-1 (-)	1.03E+0 (-)	9.99E-1 (-)
DTLZ2	5	2.123E-1	2.292E-1 (-)	2.389E-1 (-)	2.307E-1 (-)	2.302E-1 (-)	2.386E-1 (-)
		9.99E-1	9.98E-1 (-)	9.89E-1 (-)	9.91E-1 (-)	9.96E-1 (-)	9.88E-1 (-)
	10	4.616E-1	4.811E-1 (-)	4.712E-1 (-)	5.183E-1 (-)	5.712E-1 (-)	5.109E-1 (-)
		1.00E+0	9.99E-1 (=)	9.98E-1 (-)	9.73E-1 (-)	9.78E-1 (-)	9.86E-1 (-)
	15	5.689E-1	<u>5.807E-1 (-)</u>	5.990E-1 (-)	6.199E-1 (-)	7.516E-1 (-)	6.123E-1 (-)
		9.89E-1	9.73E-1 (-)	9.70E-1 (-)	9.53E-1 (-)	9.44E-1 (-)	9.65E-1 (-)
DTLZ3	5	1.695E-1	<u>1.716E-1 (-)</u>	1.983E-1 (-)	2.820E-1 (-)	1.816E-1 (-)	3.898E-1 (-)
		1.05E+0	1.01E+0 (-)	9.96E-1 (-)	9.71E-1 (-)	9.97E-1 (-)	9.26E-1 (-)
	10	4.598E-1	<u>4.617E-1 (-)</u>	4.788E-1 (-)	4.703E-1 (-)	4.726E-1 (-)	5.223E-1 (-)
		1.03E+0	1.00E+0 (-)	9.92E-1 (-)	9.98E-1 (-)	9.94E-1 (-)	9.69E-1 (-)
	15	5.993E-1	<u>6.126E-1 (-)</u>	6.936E-1 (-)	6.882E-1 (-)	7.109E-1 (-)	6.233E-1 (-)
		9.97E-1	9.94E-1 (-)	9.68E-1 (-)	9.29E-1 (-)	9.21E-1 (-)	9.86E-1 (-)
DTLZ4	5	1.680E-1	<u>1.692E-1 (=)</u>	1.726E-1 (-)	1.795E-1 (-)	2.378E-1 (-)	2.531E-1 (-)
		1.09E+0	1.07E+0 (-)	9.90E-1 (-)	9.84E-1 (-)	9.62E-1 (-)	9.63E-1 (-)
	10	4.276E-1	4.286E-1 (-)	4.622E-1 (-)	<u>4.283E-1 (+)</u>	4.596E-1 (-)	5.690E-1 (-)
		9.99E-1	9.97E-1 (-)	9.91E-1 (-)	9.95E-1 (-)	9.86E-1 (-)	9.75E-1 (-)
	15	3.996E-1	<u>4.223E-1 (-)</u>	4.907E-1 (-)	4.386E-1 (-)	5.116E-1 (-)	5.396E-1 (-)
		1.08E+0	1.06E+0 (-)	9.89E-1 (-)	1.00E+0 (-)	9.77E-1 (-)	9.70E-1 (-)
WFG2	5	7.398E-1	<u>7.413E-1 (-)</u>	8.117E-1 (-)	3.209E+0 (-)	7.996E-1 (-)	8.345E-1 (-)
		9.97E-1	9.94E-1 (-)	9.83E-1 (-)	9.69E-1 (-)	9.88E-1 (-)	9.84E-1 (-)
	10	1.279E-1	<u>1.283E-1 (-)</u>	1.316E-1 (-)	1.623E+0 (-)	1.356E-1 (-)	1.342E-1 (-)
		1.00E+0	9.99E-1 (-)	9.92E-1 (-)	7.87E-1 (-)	9.77E-1 (-)	9.85E-1 (-)
	15	1.189E-1	<u>1.222E-1 (=)</u>	1.324E-1 (-)	1.612E-1 (-)	1.637E+0 (-)	1.647E-1 (-)
		9.91E-1	9.86E-1 (-)	9.74E-1 (-)	9.70E-1 (-)	9.38E-1 (-)	9.61E-1 (-)
WFG3	5	4.896E-1	5.101E-1 (-)	5.221E-1 (-)	5.117E-1 (-)	4.870E-1 (+)	7.711E-1 (-)
		7.47E-1	7.41E-1 (=)	7.26E-1 (-)	7.34E-1 (-)	7.48E-1 (+)	6.42E-1 (-)
	10	1.115E-1	<u>1.123E-1 (-)</u>	1.126E-1 (-)	1.234E-1 (-)	1.174E-1 (-)	1.311E+0 (-)
		8.39E-1	8.33E-1 (-)	8.27E-1 (-)	8.19E-1 (-)	8.20E-1 (-)	6.78E-1 (-)
	15	3.196E+0	<u>3.226E+0 (-)</u>	3.234E+0 (-)	4.101E+0 (-)	3.486E+0 (-)	3.839E+0 (-)
		5.91E-1	5.79E-1 (-)	5.71E-1 (-)	5.16E-1 (-)	5.86E-1 (+)	5.67E-1 (-)
WFG5	5	6.298E-1	<u>6.464E-1 (-)</u>	7.186E-1 (-)	9.912E-1 (-)	7.229E-1 (-)	7.236E-1 (-)
		8.73E-1	8.61E-1 (-)	8.27E-1 (-)	7.49E-1 (-)	8.17E-1 (-)	8.16E-1 (-)
	10	5.856E-1	<u>5.937E-1 (-)</u>	1.598E+0 (-)	1.221E+0 (-)	7.823E-1 (-)	3.909E+0 (-)
		1.08E+0	1.07E+0 (-)	5.69E-1 (-)	5.18E-1 (-)	1.05E+0 (-)	4.76E-1 (-)
	15	1.056E-1	<u>1.068E-1 (-)</u>	2.221E+0 (-)	2.118E+0 (-)	4.685E+0 (-)	1.286E+0 (-)
		5.32E-1	<u>5.34E-1 (=)</u>	4.68E-1 (-)	4.06E-1 (-)	2.31E-1 (-)	4.51E-1 (-)
WFG9	5	3.254E-1	<u>3.385E-1 (-)</u>	4.616E-1 (-)	4.128E-1 (-)	9.111E-1 (-)	3.487E-1 (-)
		9.91E-1	9.87E-1 (-)	9.53E-1 (-)	9.64E-1 (-)	7.46E-1 (-)	9.80E-1 (-)
	10	6.163E-1	<u>6.213E-1 (-)</u>	6.235E-1 (-)	6.594E-1 (-)	6.919E-1 (-)	6.783E-1 (-)
		9.33E-1	9.27E-1 (-)	9.11E-1 (-)	8.87E-1 (-)	8.93E-1 (-)	8.81E-1 (-)
	15	7.992E+0	<u>8.129E+0 (-)</u>	8.386E+0 (-)	8.207E+0 (-)	1.118E+1 (-)	1.382E+1 (-)
		3.69E-1	3.64E-1 (-)	3.51E-1 (-)	3.57E-1 (-)	2.67E-1 (-)	2.65E-1 (-)
MaF1	5	1.146E-1	<u>1.211E-1 (-)</u>	3.256E-1 (-)	3.036E-1 (-)	1.429E-1 (-)	1.252E-1 (-)
		9.27E-3	9.13E-3 (-)	2.00E-3 (-)	2.24E-3 (-)	7.91E-3 (-)	8.82E-3 (-)
	10	2.261E-1	2.250E-1 (+)	5.352E-1 (-)	6.849E-1 (-)	6.972E-1 (-)	2.317E-1 (-)
		5.83E-7	5.80E-7 (-)	7.32E-9 (-)	5.86E-9 (-)	5.91E-9 (-)	5.81E-7 (-)
	15	2.415E-1	<u>2.531E-1 (-)</u>	6.934E-1 (-)	7.120E-1 (-)	5.928E-1 (-)	3.164E-1 (-)
		9.99E-11	<u>9.97E-11 (-)</u>	1.60E-13 (-)	2.90E-14 (-)	3.66E-14 (-)	8.00E-13 (-)
MaF3	5	9.623E-2	1.024E-1 (-)	<u>9.463E-2 (-)</u>	9.358E-2 (+)	2.594E-1 (-)	2.599E-1 (-)
		9.53E-1	9.26E-1 (-)	9.60E-1 (-)	9.80E-1 (+)	8.73E-1 (-)	8.87E-1 (-)
	10	8.126E-2	<u>8.389E-2 (-)</u>	1.288E-1 (-)	1.338E-1 (-)	1.088 E+0 (-)	9.821E-1 (-)
		9.99E-1	9.98E-1 (-)	9.87E-1 (-)	9.78E-1 (-)	1.11E-1 (-)	9.87E-1 (-)
	15	8.194E-2	<u>8.337E-2 (-)</u>	9.326E-2 (-)	9.984E-2 (-)	9.598E-1 (-)	2.883E-1 (-)
		9.99E-1	9.96E-1 (-)	9.76E-1 (-)	9.95E-1 (-)	9.94E-1 (-)	8.31E-1 (-)
MaF6	5	9.222E-3	9.394E-3 (-)	8.331E-2 (-)	9.505E-3 (-)	9.191E-3 (-)	1.923E-1 (-)
		1.16E-1	1.12E-1 (-)	1.08E-1 (-)	1.01E-1 (-)	1.18E-1 (-)	1.07E-1 (-)
	10	3.112E-3	<u>3.182E-3 (-)</u>	3.341E-1 (-)	1.010E-1 (-)	4.154E-3 (-)	7.728E-1 (-)
		1.06E-1	1.00E-1 (-)	1.04E-1 (-)	7.91E-2 (-)	9.83E-2 (-)	4.35E-2 (-)
	15	9.635E-2	<u>9.710E-2 (-)</u>	9.992E-2 (-)	2.008E-1 (-)	9.915E-2 (-)	3.616E-1 (-)
		9.67E-2	9.63E-2 (-)	9.57E-2 (-)	8.73E-2 (-)	9.41E-2 (-)	8.66E-2 (-)
MaF7	5	3.213E-1	3.366E-1 (-)	4.508E-1 (-)	4.601E-1 (-)	2.998E-1 (+)	5.468 E-1 (-)
		2.53E-1	2.51E-1 (-)	2.49E-1 (-)	2.43E-1 (-)	2.56E-1 (+)	2.12E-1 (-)
	10	8.218E-1	<u>8.686E-1 (-)</u>	8.462E-1 (-)	2.122E+0 (-)	8.693E-1 (-)	1.889E+0 (-)
		1.86E-1	1.65E-1 (-)	1.84E-1 (=)	1.46E-1 (-)	1.95E-1 (-)	1.51E-1 (-)
	15	2.126E+0	<u>2.387E+0 (-)</u>	2.661E+0 (-)	4.022E+0 (-)	6.659E+0 (-)	2.399E+0 (-)
		1.72E-1	<u>1.57E-1 (-)</u>	1.53E-1 (-)	6.13E-2 (-)	3.16E-2 (-)	1.55E-1 (-)
IGD: +/-/=		-	1/33/2	0/36/0	2/34/0	2/34/0	0/36/0
HV: +/-/=		-	0/33/3	0/35/1	1/35/0	3/33/0	0/36/0

Table 3: Results of the Friedman and Iman-Davenport tests in terms of IGD and HV ($\alpha = 0.05$).

Test	Parameters		Null hypothesis	p-value
	Crit. value	Value		
IGD				
Friedman	11.07	107.492	Rejected	1.388E-21
Iman-Davenport	2.27	51.887	Rejected	1.110E-16
HV				
Friedman	11.07	107.184	Rejected	1.612E-21
Iman-Davenport	2.27	51.419	Rejected	1.110E-16

35, 33, and 36 problems from a total of 36 test instances in terms of the HV. Table 3 shows the obtained results of the Friedman and Iman-Davenport tests for the IGD and HV performance indicators. In fact, with a level of significance $\alpha = 0.05$, the obtained values by both statistical tests are clearly larger than their associated critical values. Therefore, there are significant differences among the obtained results and the null hypothesis is rejected. Thus, our proposed ANBID-DEA performs significantly better than all the other compared approaches.

This superior performance of our proposed ANBID-DEA is mainly due to the following aspects: (1) we use the NBI directions that uniformly intersect the PF regardless of its geometrical shape, (2) we adaptively update the NBI directions during the search process to cover the non-discovered parts of the PF with some solutions, and (3) we ensure a balance between convergence and diversity by considering the importance of preserving isolated solutions and adopting the Euclidean and acute angle mechanisms in our proposed worse-elimination selection mechanism. For all these reasons, our proposed ANBID-DEA is able to outperform the other algorithms with respect to which it was compared when dealing with high dimensional problems with complex PFs.

6 Conclusions and Future Work

This paper introduced ANBID-DEA, a new decomposition-based algorithm that adaptively updates the NBI directions used in MP-DEA when applying its enhanced worse-elimination selection mechanism. An empirical study was carried out to evaluate the performance of ANBID-DEA on a set of selected many-objective unconstrained benchmark problems with irregular PFs and with a number of objectives that goes from 5 to 15. The obtained results showed that our proposed approach is competitive when compared against five state-of-the-art algorithms on the majority of the test instances adopted. As part of our future work, we are interested in designing an efficient constraint-handling technique and integrate it into ANBID-DEA [22]. We are also interested in the development of a surrogate-assisted evolutionary algorithm to solve expensive MaOPs where a small number of real-objective function evaluations are allowed [10]. Finally, we are also interested in applying machine learning methods to solve MaOPs [20].

References

1. Bao, C., Gao, D., Gu, W., Xu, L., Goodman, E.D.: A new adaptive decomposition-based evolutionary algorithm for multi- and many-objective optimization. *Expert Systems with Applications* **213**, 119080 (2023)
2. Bosman, P.A., Thierens, D.: The balance between proximity and diversity in multi-objective evolutionary algorithms. *IEEE Transactions on Evolutionary Computation* **7**(2), 174–188 (2003)
3. Cheng, R., Jin, Y., Olhofer, M., Sendhoff, B.: A reference vector guided evolutionary algorithm for many-objective optimization. *IEEE Transactions on Evolutionary Computation* **20**(5), 773–791 (2016)
4. Deb, K., Jain, H.: An evolutionary many-objective optimization algorithm using reference-point-based nondominated sorting approach, part I: Solving problems with box constraints. *IEEE Transactions on Evolutionary Computation* **18**(4), 577–601 (2014)
5. Elarbi, M., Bechikh, S., Ben Said, L., Datta, R.: Multi-objective optimization: Classical and evolutionary approaches. *Recent advances in evolutionary multi-objective optimization* pp. 1–30 (2017)
6. Elarbi, M., Bechikh, S., Coello, C.A.C., Makhoul, M., Said, L.B.: Approximating complex Pareto fronts with predefined normal-boundary intersection directions. *IEEE Transactions on Evolutionary Computation* **24**(5), 809–823 (2019)
7. Giagkiozis, I., Purshouse, R.C., Fleming, P.J.: Towards understanding the cost of adaptation in decomposition-based optimization algorithms. In: 2013 IEEE International Conference on Systems, Man, and Cybernetics. pp. 615–620. IEEE (2013)
8. Gu, F., Cheung, Y.M.: Self-organizing map-based weight design for decomposition-based many-objective evolutionary algorithm. *IEEE Transactions on Evolutionary Computation* **22**(2), 211–225 (2017)
9. Guo, X.: A survey of decomposition based evolutionary algorithms for many-objective optimization problems. *IEEE Access* **10**, 72825–72838 (2022)
10. He, C., Cheng, R., Jin, Y., Yao, X.: Surrogate-assisted expensive many-objective optimization by model fusion. In: 2019 IEEE congress on evolutionary computation (CEC). pp. 1672–1679. IEEE (2019)
11. Jain, H., Deb, K.: An evolutionary many-objective optimization algorithm using reference-point based nondominated sorting approach, part II: Handling constraints and extending to an adaptive approach. *IEEE Transactions on evolutionary computation* **18**(4), 602–622 (2013)
12. Li, K.: A survey of multi-objective evolutionary algorithm based on decomposition: Past and future. *IEEE Transactions on Evolutionary Computation* (2024). <https://doi.org/10.1109/TEVC.2024.3496507>
13. Li, K., Deb, K., Zhang, Q., Kwong, S.: An evolutionary many-objective optimization algorithm based on dominance and decomposition. *IEEE Transactions on Evolutionary Computation* **19**(5), 694–716 (2015)
14. Li, M., Yao, X.: What weights work for you? Adapting weights for any Pareto front shape in decomposition-based evolutionary multi-objective optimisation. *Evolutionary Computation* **28**(2), 227–253 (2020)
15. Liu, H.L., Chen, L., Zhang, Q., Deb, K.: Adaptively allocating search effort in challenging many-objective optimization problems. *IEEE Transactions on Evolutionary Computation* **22**(3), 433–448 (2017)
16. Liu, Q., Jin, Y., Heiderich, M., Rodemann, T.: Adaptation of reference vectors for evolutionary many-objective optimization of problems with irregular Pareto

- fronts. In: 2019 IEEE Congress on Evolutionary Computation (CEC). pp. 1726–1733. IEEE (2019)
17. Liu, Q., Jin, Y., Heiderich, M., Rodemann, T., Yu, G.: An adaptive reference vector-guided evolutionary algorithm using growing neural gas for many-objective optimization of irregular problems. *IEEE Transactions on Cybernetics* **52**(5), 2698–2711 (2020)
 18. Ma, X., Yu, Y., Li, X., Qi, Y., Zhu, Z.: A survey of weight vector adjustment methods for decomposition-based multiobjective evolutionary algorithms. *IEEE Transactions on Evolutionary Computation* **24**(4), 634–649 (2020)
 19. Qi, Y., Ma, X., Liu, F., Jiao, L., Sun, J., Wu, J.: MOEA/D with adaptive weight adjustment. *Evolutionary Computation* **22**(2), 231–264 (2014)
 20. Qu, Q., Ma, Z., Clausen, A., Jørgensen, B.N.: A comprehensive review of machine learning in multi-objective optimization. In: 2021 IEEE International Conference on Big Data and Artificial Intelligence (BDAI). pp. 7–14. IEEE (2021)
 21. Sato, H.: Analysis of inverted PBI and comparison with other scalarizing functions in decomposition based MOEAs. *Journal of Heuristics* **21**, 819–849 (2015)
 22. Sharma, A.K., Datta, R., Elarbi, M., Bhattacharya, B., Bechikh, S.: Practical applications in constrained evolutionary multi-objective optimization. *Recent advances in evolutionary multi-objective optimization* pp. 159–179 (2017)
 23. Sheskin, D.J.: *Handbook of parametric and nonparametric statistical procedures*. Chapman and hall/CRC (2003)
 24. Tian, Y., Cheng, R., Zhang, X., Jin, Y.: PlatEMO: A MATLAB platform for evolutionary multi-objective optimization [educational forum]. *IEEE Computational Intelligence Magazine* **12**(4), 73–87 (2017)
 25. Wu, M., Li, K., Kwong, S., Zhang, Q., Zhang, J.: Learning to decompose: A paradigm for decomposition-based multiobjective optimization. *IEEE Transactions on Evolutionary Computation* **23**(3), 376–390 (2018)
 26. Xiang, Y., Zhou, Y., Li, M., Chen, Z.: A vector angle-based evolutionary algorithm for unconstrained many-objective optimization. *IEEE Transactions on Evolutionary Computation* **21**(1), 131–152 (2016)
 27. Xu, Y., Li, F., Zhang, H., Li, W.: An adaptive reference vector guided many-objective optimization algorithm based on the Pareto front density estimation. *Swarm and Evolutionary Computation* **88**, 101601 (2024)
 28. Yuan, Y., Xu, H., Wang, B., Yao, X.: A new dominance relation-based evolutionary algorithm for many-objective optimization. *IEEE Transactions on Evolutionary Computation* **20**(1), 16–37 (2015)
 29. Zhang, Q., Li, H.: MOEA/D: A multiobjective evolutionary algorithm based on decomposition. *IEEE Transactions on Evolutionary Computation* **11**(6), 712–731 (2007)
 30. Zhang, Z., Gao, S., Lei, Z., Xiong, R., Cheng, J.: Pareto dominance archive and co-ordinated selection strategy-based many-objective optimizer for protein structure prediction. *IEEE/ACM Transactions on Computational Biology and Bioinformatics* **20**(3), 2328–2340 (2023)
 31. Zhang, Z., Zhao, M., Wang, H., Cui, Z., Zhang, W.: An efficient interval many-objective evolutionary algorithm for cloud task scheduling problem under uncertainty. *Information Sciences* **583**, 56–72 (2022)
 32. Zitzler, E., Thiele, L.: Multiobjective evolutionary algorithms: A comparative case study and the strength pareto approach. *IEEE Transactions on Evolutionary Computation* **3**(4), 257–271 (1999)